European Journal of Cell Biology 104 (2025) 151521

Contents lists available at ScienceDirect

European Journal of Cell Biology

journal homepage: www.elsevier.com/locate/ejcb

Deciphering the landscape of post-translational modifications in the centrosome upon T cell activation

Marta Lozano-Prieto [a,b,1], Inmaculada Jorge [b,c,1], Emilio Camafeita [b,c], Cristina A. Devesa [c], Rafael Barrero-Rodríguez [c], Enrique Calvo [b,c], Andrea Laguillo-Gómez [c], Clara Pertusa [a], Noa B. Martin-Cofreces [a,b,e,*], Jesús Vázquez [b,c,**], Francisco Sánchez-Madrid [a,b,d,***]

[a] Immunology Service, Hospital Universitario de la Princesa, Instituto Investigación Sanitaria Princesa (IIS-IP), Madrid, Spain
[b] Centro de Investigación Biomédica en Red, Enfermedades Cardiovasculares (CIBERCV), Madrid, Spain
[c] Cardiovascular Proteomics Laboratory, Centro Nacional de Investigaciones Cardiovasculares Carlos III (CNIC), Madrid, Spain
[d] Universidad Autónoma de Madrid (UAM), Madrid, Spain
[e] Videomicroscopy Unit, Instituto de Investigación Sanitaria La Princesa (IIS-Princesa), Madrid, Spain

ARTICLE INFO

Keywords:
Post-translational modifications
Centrosome
T lymphocytes
Proteomics

ABSTRACT

The shift from quiescent to effector T cells (TC) is controlled at the translational level. Post-translational modifications (PTMs) are key factors in the diversification of protein function. Advancements in mass spectrometry-based proteomics enable proteome-wide, hypothesis-free quantitative PTM analysis. Current research highlights the centrosome role in TC activation. Here the diversity of PTMs in the TC centrosome is studied by analyzing centrosome-enriched fractions from human resting and activated T lymphoblasts. Our results show that oxidative modifications predominate in this organelle, with tryptophan as the most frequently oxidized residue. These PTMs are enriched in proteins involved in translation, vesicular trafficking, cytoskeleton organization, among others. We also demonstrate the existence of PTM changes on specific protein regions during TC activation in Myh9 (hyperoxidized), and Gzma (hypoxidized). These hyper- or hypoxidized proteins display distinct functional distributions. Our study provides the first comprehensive PTM mapping of the TC centrosome, underscoring the PTM regulatory role in TC activation.

1. Introduction

T cell activation is critical to immune responses and has been studied extensively. Recent research shows that the transition from resting to effector T cells is tightly regulated at the translational level (Ricciardi et al., 2018; Wolf et al., 2020; Howden et al., 2019). Resting T lymphocytes maintain a primed state, allowing them to rapidly respond to new threats by storing specific mRNA and keeping a pool of idle ribosomes ready for swift protein synthesis upon activation (Ricciardi et al., 2018; Wolf et al., 2020; Jurgens et al., 2021). It is worth noting that in human CD4 T lymphocytes there is no correlation between transcription and translation during early activation, although correlation increases during the process of differentiation into subsets from naïve and memory cells (Cano-Gamez et al., 2020). Moreover, previous studies in mouse T cells also point to differences in the transcriptomics and proteomics profiles during TCR activation (Tan et al., 2017; Dybas

Abbreviations: PTMs, Post-translational modifications; OS, Open search; LC-MS/MS, Liquid chromatography - tandem mass spectrometry; JK, Jurkat E6-1 human T cells; HEK, Human embryonic kidney 293 cells; LT CTRL, Resting human T lymphoblasts; LT ACT, Activated human T lymphoblasts; PIPES, Piperazine-N,N-bis2-ethanesulfonic acid; PBLs, Peripheral blood lymphocytes; SEE, Staphylococcus enterotoxin E; PHA, Phytohaemagglutinin; HBSS, Hank's balanced salt solution; IL-2, Interleukin-2; SPD, Samples per day; ITRAQ, Isobaric tag for relative and absolute quantitation; PSM, Peptide-spectrum match; ACN, Acetonitrile; FC, Fold change; NM, Non-modified; Myh9, Myosin heavy chain 9; Gzma, Granzyme A; IDO, Indoleamine 2,3-dioxygenase; IFN-γ, Interferon-gamma; ROS, Reactive oxygen species; RNS, Reactive nitrogen species; TCR, T cell receptor.

* Corresponding author at: Videomicroscopy Unit, Instituto de Investigación Sanitaria La Princesa (IIS-Princesa), Madrid, Spain.
** Corresponding author at: Cardiovascular Proteomics Laboratory, Centro Nacional de Investigaciones Cardiovasculares Carlos III (CNIC), Madrid, Spain.
*** Correspondence to: Hospital Universitario de la Princesa Immunology Unit, Calle Diego de León 62, Madrid, Spain.
E-mail addresses: noa.martin@salud.madrid.org (N.B. Martin-Cofreces), jesus.vazquez@cnic.es (J. Vázquez), fsmadrid@salud.madrid.org (F. Sánchez-Madrid).

[1] These authors contributed equally to this work.

https://doi.org/10.1016/j.ejcb.2025.151521
Received 8 July 2025; Received in revised form 10 September 2025; Accepted 30 September 2025
Available online 1 October 2025
0171-9335/

et al., 2019). These findings underscore the importance of investigating the molecular processes driving T cell activation at the translational level. Remarkably, the centrosome is a key player in the organization and polarization processes during T cell activation (Martín-Cófreces et al., 2008). It has been shown that the cytosolic CCT chaperonin, among other proteins, increases in centrosomes from activated T cells, affecting their response to TCR/CD28 stimulation (Martin-Cofreces et al., 2020). These findings highlight the relevance of the centrosome in T cell activation.

Protein post-translational modifications (PTMs) exponentially expand proteome complexity and play crucial roles in regulating protein localization, activity, folding, interactions, and stability. In line with their functional relevance, a pivotal role of PTMs has been found in various conditions such as cancer (Liu et al., 2021), neurodegeneration (Alquezar et al., 2021; Junqueira et al., 2019), and cardiovascular disease (Noels et al., 2024). As a result, PTMs are increasingly gaining attention as potential biomarkers for diagnosis, prognosis and treatment of certain conditions. However, true hypothesis-free analysis of PTMs was not possible until relatively recently with the development of the open search (OS) strategy (Chick et al., 2015), which enabled the identification of any peptidoform detected by liquid chromatography - tandem mass spectrometry (LC-MS/MS) analysis by using peptide precursor mass tolerance of hundreds of Da. This approach was later refined to pinpoint modification sites (Bagwan et al., 2018; Yu et al., 2020), and a quantitative statistical model, based on the Generic Integration Algorithm (García-Marqués et al., 2016), has been specifically designed for high-throughput analysis of post-translationally modified peptides (Bagwan et al., 2018). Based on the flexibility of the open-source package iSanXoT (Rodríguez et al., 2023; Trevisan-Herraz et al., 2019) to adapt quantitative PTM workflows to any type of proteomics experiment, this approach has been applied in several unbiased, proteome-wide PTM studies in the context of heteroplasmy (Bagwan et al., 2018; Lechuga-Vieco et al., 2022), and cardiovascular disease (Martínez-López et al., 2019; Ruiz-Meana et al., 2019; de la Fuente-Alonso et al., 2021; Binek et al., 2024), among others.

In this work we have resorted to Comet-PTM and iSanXoT to provide the first comprehensive description of the complex landscape of PTMs in the centrosome upon T cell activation. Understanding the role of these modifications will provide valuable insights into the molecular mechanisms driving immune responses and could pave the way for the development of novel therapeutic strategies.

2. Material and methods

2.1. MS data

2.1.1. Experimental design

In this work we analyzed two proteomic datasets. Dataset 1 included proteomics data from centrosome-enriched fractions of Jurkat E6–1 human T cells (JK), human embryonic kidney (HEK) 293 cells, resting human T lymphoblasts (LT CTRL) and activated human T lymphoblasts (LT ACT), with one biological replicate for each condition. Dataset 2 included proteomics data from centrosome-enriched fractions from resting and activated T lymphoblasts from thirty healthy donors. Both datasets were taken from previously published MS data, detailed in Lozano-Prieto et al. (2024) and Martin-Cofreces et al. (2020), respectively. Dataset 1 was conceived as an exploratory and descriptive study aimed at broadly characterizing the PTM landscape in the centrosome. Its findings guided the design of the subsequent, quantitatively robust analysis using samples from thirty donors (Dataset 2), which included appropriate biological replication for statistical analysis.

2.2. Dataset 1

2.2.1. Sample collection

2.2.1.1. Jurkat E6-1 human T cell (JK) centrosomes. Centrosome-enriched subcellular fractions from JK cells were prepared as described in Lozano-Prieto et al. (2024). Briefly, cells were cooled on ice, centrifuged, washed with Tris-buffered saline, and resuspended in lysis buffer (2×10^6 cells/ml) containing protease and phosphatase inhibitors. After gentle shaking, lysates were filtered through a nylon mesh and centrifuged. The supernatant was re-equilibrated into piperazine-N,N-bis (2-ethanesulfonic acid) (PIPES) (pH 7.2) and centrifuged again to pellet centrosomes. The pellet was resuspended in gradient buffer, homogenized, and subjected to two rounds of sucrose gradient centrifugation. Fractions were collected and analyzed for γ-tubulin content by Western blot and total protein quantification using the BCA Protein Assay.

2.2.1.2. Human embryonic kidney (HEK) 293 cell centrosomes. Centrosome-enriched subcellular fractions from HEK 293 cells were prepared as described in Lozano-Prieto et al. (2024). HEK 293 cells were scraped from cell culture plates and 10^9 cells were processed as described above to isolate centrosome-enriched fractions.

2.2.1.3. Human resting and activated T lymphoblast (LT CTRL and LT ACT) centrosomes. Centrosome-enriched subcellular fractions from LT CTRL and LT ACT were prepared as described in Lozano-Prieto et al. (2024). Briefly, peripheral blood lymphocytes (PBLs) were isolated from buffy coats using a Ficoll gradient and depleted of monocytes through an adhesion step. The PBLs were activated with Staphylococcus enterotoxin E (SEE) and phytohaemagglutinin (PHA) for 48 h. After washing with Hank's balanced salt solution (HBSS), cells were cultured in medium containing interleukin-2 (IL-2) for 7–10 days. Cells were split and stimulated with either anti-CD3ε and anti-CD28-coated beads (LT ACT) or control gamma-globulin-coated beads (LT CTRL) for 15–20 min. Cells were ice-cooled and subjected to the centrosome-enriched fraction isolation procedure as described above.

To note, no B cell depletion or CD3⁺ selection was performed. However, our sequential culture conditions strongly disfavor persistent B cell survival and expansion: PHA and SEE activate T cells but do not directly drive B cell proliferation (Geha et al., 1974); IL-2 alone does not sustain B cells unless pre-activated via BCR/CD40; and prior monocyte removal limits BAFF-dependent B cell survival. Late IL-2 supplementation after mitogen and superantigen priming is a standard approach to generate T cell blasts from PBMCs (Kennell et al., 2014). Although a transient presence of B cells early in culture cannot be excluded, these conditions make a meaningful B cell contribution to our centrosome PTM profiles unlikely.

2.2.2. Preparation of protein extracts

Protein extracts were prepared as described in Lozano-Prieto et al. (2024). In brief, centrosome preparations were boiled in a lysis buffer, centrifuged and the supernatants were collected. Protein concentrations were measured using the RC DC protein assay kit (BioRad) according to the manufacturer's instructions.

2.2.3. On-filter protein digestion

Digestion of samples was performed as previously detailed in Lozano-Prieto et al. (2024). Briefly, protein extracts were combined with denaturing buffer and concentrated using 30 K FASP filters (Expedeon). Samples were washed with denaturing buffer and free thiol groups were alkylated by iodoacetamide incubation. Filters were washed with denaturing buffer followed by a wash with trypsin digestion buffer. Proteins were digested using trypsin (Promega, Madison, WI, USA). Tryptic peptides were collected by centrifugation, acidified with trifluoroacetic acid, desalted using C18 Oasis HLB extraction cartridges, and subsequently dried.

2.2.4. LC-MS/MS analysis

LC-MS/MS analysis was done using an Evosep One HPLC (Evosep, Odense, Denmark) coupled to an Orbitrap Eclipse Tribrid Mass Spectrometer (Thermo Fisher Scientific) using an Endurance Evosep column 15 cm× 150 µm ID as analytical column (Thermo Fisher Scientific) coupled to a stainless steel emitter of 30 µm ID. Peptides were eluted from Evotips and analyzed using the Evosep One pre-programmed gradient for 15 samples per day (SPD). Mass spectra were acquired in data-dependent manner, with an automatic switch between MS and MS/MS with a 2 s cycle time Top Speed method and 40 s dynamic exclusion. For further details, refer to Lozano-Prieto et al. (2024).

2.3. Dataset 2

2.3.1. Sample collection

Centrosome-enriched subcellular fractions from LT CTRL and LT ACT were prepared as described above (section 2.2.1.3). Samples from different donors were pooled after first lysis. For further details, refer to Martin-Cofreces et al. (2020).

2.3.2. Preparation of protein extracts

Protein extracts were prepared as described above (section 2.2.2). For further details, refer to Martin-Cofreces et al. (2020).

2.3.3. In-gel digestion and sample labelling

Protein samples were digested and labelled as described in Martin-Cofreces et al. (2020). Proteins were digested using an in-gel digestion protocol, which involved SDS-PAGE separation, colloidal Coomassie staining, band excision, reduction, alkylation, and overnight trypsin digestion. The resulting peptides were extracted, acidified with trifluoroacetic acid, desalted using C18 Oasis HLB extraction cartridges, and dried-down.

For multiplexed isobaric labeling, three separate experiments were conducted, each including two biological replicates per condition, and analyzed using three independent iTRAQ 4-plex assays. Peptides were quantified and labelled with reagents according to the iTRAQ 4-plex manufacturer's protocol (Applied Biosystems, Foster City, CA, USA). Labelled peptides were combined, desalted, and fractionated using mixed-cation exchange chromatography.

2.3.4. LC-MS/MS analysis

LC-MS/MS analysis was done using an UPLC-Ultimate 3000 (Thermo Fisher Scientific) coupled to a Q exactive mass spectrometer (Thermo Fisher Scientific) using a PepMap 100 C18 0.3 × mm 5 mm ID as trapping column (Thermo Fisher Scientific) and a PepMap RSLC C18 EASY-Spray column 50 cm× 75 µm ID as analytical column (Thermo Fisher Scientific). Labelled peptides were loaded in buffer A (0.1 % of formic acid in water (v/v)) and eluted with a 360 min linear gradient of buffer B (100 % ACN, 0.1 % formic acid (v/v)) at 200 nL/min. Mass spectra were acquired in data-dependent manner, with an automatic switch between MS and MS/MS with a "Top-15" method and 30 s dynamic exclusion. For further details, refer to Martin-Cofreces et al. (2020).

3. MS data analysis

3.1. PTM open search

The Thermo Scientific LC-MS/MS RAW files were converted to the mzML format using ThermoRawFileParser version 1.1.9 (Hulstaert et al., 2020). The mzML MS data were open-searched against a human UniProt (May 2021) concatenated target-decoy database with Comet-ReCom (Laguillo-Gómez et al., 2023) using the following parameters: one maximum trypsin missed cleavage site, 500 Da precursor mass tolerance, 0.02 Da fragment mass tolerance. Cys carbamidomethylation was in all cases considered as a fixed modification. Additionally, in the case of the samples from dataset 2 (see Subsection 2.3 above), 144.102063 Da (iTRAQ 4-plex) was set as fixed modifications at Lys and peptide N-terminus. MS data analyses were performed using the PTM-compass application, as described in Devesa et al. (2025) [preprint], and PSM peak, local, and global false discovery rates (FDR) were calculated. The Unimod database was used to associate the mass shifts (Δmass values) detected with known PTMs. Notably, no PTM classes were selected *a priori* for their assessment. The PTM search was unbiased, and the posterior analysis reflects the most abundant, confidently localized, Unimod-annotated PTMs observed in the centrosome enriched samples.

3.2. Statistical rationale

To detect significantly associated modification-amino acid pairs, we performed an enrichment test based on the binomial distribution with Dataset 1. Under the null hypothesis of no association, the expected proportion of a given modification-amino acid pair occurring by chance alone was estimated as the product of the observed proportion of the modification and the observed proportion of the amino acid, considering only residues within ±5 positions around PTM sites in the dataset. Then, the statistical significance that each observed modification-amino acid pair is encountered with a frequency higher than the expected one was assessed using the binomial test and the expected proportion of the modification-amino acid pair. The analysis was conducted at PSM (peptide-spectrum match) level, with p-values adjusted for multiple testing, using the Benjamini-Hochberg procedure. Enrichments with q-values < 0.01 were deemed statistically significant to assess highly reliable PTM-residue associations.

Dataset 1 was subjected to enrichment analysis for proteins containing oxidative PTM using a hypergeometric test and considering PSM as a measure of abundance. Only proteins with more than five PSMs of oxidative PTMs were considered. The test uses the total abundance of proteins (M) and of oxidative PTMs (n) in each proteome, and the abundance of the protein (N) and of its oxidative PTMs (k). The hypergeometric test was applied to assess the probability of observing k or more PSMs of oxidative PTMs for a given protein by chance. The resulting p-values were adjusted for multiple comparisons using the Benjamini-Hochberg method and enrichments with q-values < 0.05 were considered statistically significant. The fold change (FC) was calculated as the ratio of observed (k) to expected ((N/M)*n) PSMs of oxidative PTMs and expressed on a logarithmic scale.

Dataset 2 was subjected to quantitative PTM analysis using the integrative multilayer workflow previously described in Devesa et al. (2025) [preprint] and iSanXoT version 1.2.12 (Rodríguez et al., 2023). This procedure allowed the detection of specific PTM abundance changes, which is not affected by the presence of artefacts, and of hypermodified peptides (Devesa et al., 2025 [preprint]). One-sample Limma test was employed, since the comparisons were performed by pairing data from activated and control lymphoblasts from the same donors to control for inter-donor variability. Methylation on glutamic acid was excluded from this dataset as it was deemed a potential artifact arising from in-gel digestion (Lozano-Prieto et al., 2024). Abundance changes with p-value < 0.05 were considered statistically significant.

To analyze the distribution of protein hypermodifications from a systems biology perspective, we calculated the difference (ΔNM) in PSM counts between non-modified (NM) peptides that were significantly (p-value < 0.05) increased and those that were significantly decreased upon lymphoblast activation:

$$\Delta NM = (\text{PSMs NM-up}) - (\text{PSMs NM-down})$$

We then measured the hypermodified protein fraction (HF) as the proportion of the difference to the total number of hypermodified peptides, that is:

HF = (PSMs NM-up - PSMs NM-down) / (PSMs NM-up + PSMs NM-down)

We considered that a protein is hyper- or hypomodified when its HF is higher than 0.4 or lower than −0.4, respectively. The top hyper/hypomodified proteins with the highest/lowest ΔNM values were selected for protein interaction network analysis followed by functional enrichment analysis using STRING.

4. Results

4.1. Centrosomal PTM map shows predominance of oxidative modifications and tryptophan as the most modified residue

To interpret the PTM map of centrosomes from Jurkat (JK), human embryonic kidney (HEK) 293 cells, resting human T lymphoblasts (LT CTRL) and activated human T lymphoblasts (LT ACT), we considered only those modifications described in the Unimod database. The results show that the vast majority of PTMs were oxidative, including mono-oxidation, di-oxidation, kynurenine, semialdehyde, quinone, tri-oxidation, oxolactone, dione, dihydroxy-N-formylkynurenine and hydroxyquinone. Methylation, phosphorylation, acetylation, di-methylation, iodination and tri-methylation were also present (see Fig. 1A-D and Supplementary Table 1). Remarkably, the four centrosomal PTM maps were very similar in terms of the types of modifications and their relative abundance, supporting the validity of our analysis and suggesting that PTMs have a common behaviour in centrosomal proteins that is cell-type independent.

We then focused on amino acids that were significantly associated to specific Δmass values (see Material and methods). PTMs were mostly located in the expected amino acids (Fig. 1E-H and Supplementary Table 2), supporting the accuracy of the PTM analysis pipeline in terms of PTM allocation. For instance, di-oxidations were assigned to Trp and Met residues, while phosphorylations were only assigned to Ser, which has been reported as the most frequently phosphorylated residue in nature (Ubersax et al., 2007). Interestingly, Trp was the most modified amino acid in the centrosome proteome. Considering the four proteomes, seven different types of modified Trp forms were present, all of them of oxidative nature: mono-oxidation, di-oxidation, tri-oxidation, kynurenine, oxolactone, dihydroxy-N-formylkynurenine and dione. Proteins modified with kynurenine and/or with a significant enrichment in this modification are listed in Supplementary Table 3 and Supplementary Figure 1.

4.2. Specific protein categories are enriched in oxidative PTMs

To get further insight into the functional implications of these PTMs and considering that oxidative modifications constituted the majority of PTMs, we investigated what type of proteins were affected by this kind of modifications. Enrichment analysis produced a list of proteins significantly enriched in oxidative modifications that partially overlapped across the four proteomes (Fig. 2A-D). From these, 33 and 56 proteins showed a significant enrichment in LT CTRL (Fig. 2B) or LT ACT (Fig. 2C), respectively, while 81 proteins were significantly enriched in oxidative PTMs in both proteomes (Fig. 2D). These proteins could be classified into ribosomal and translation machinery proteins, vesicular transport proteins, RNA binding and/or processing proteins, metabolic enzymes and mitochondrial proteins, cytoskeletal and cytoskeleton-related proteins, immune response proteins, and chromatin remodeling proteins, among others (Fig. 2B-D).

4.3. PTM dynamics upon T cell activation show different hyper- and hypomodification protein patterns

To investigate PTM dynamics in resting (LT CTRL) and activated T lymphoblasts (LT ACT) centrosomes, we assessed the differences in the abundance of modified peptidoforms. We applied an integrative multilayer workflow for PTM quantification, as described in Devesa et al.

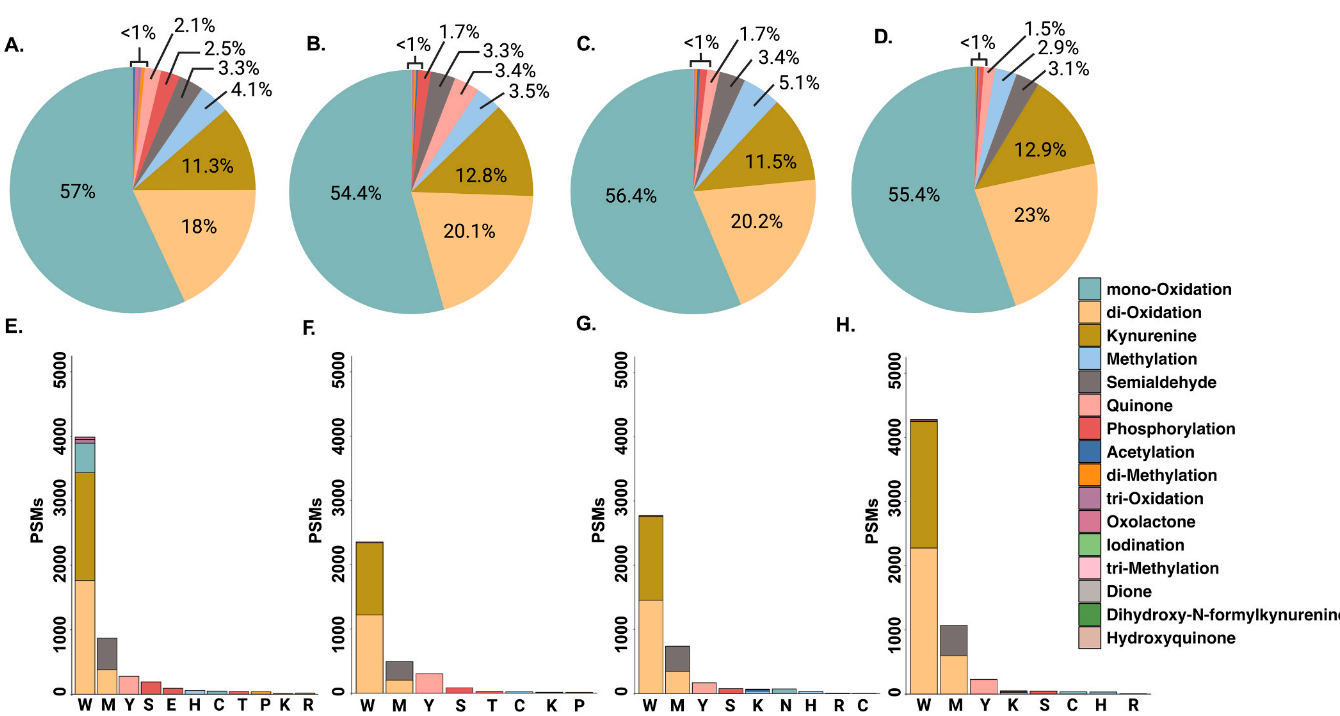

Fig. 1. Mapping of centrosome PTMs. A-D. Pie charts showing the percentages of PSMs of the known PTMs present in centrosomes. **A.** JK; **B.** HEK; **C.** LT CTRL; **D.** LT ACT. **E-H.** Stacked bar plots showing the distributions of the PTMs across the amino acids present in centrosomes. **E.** JK; **F.** HEK; **G.** LT CTRL; **H.** LT ACT. All centrosome-enriched fractions are from dataset 1. Mono-oxidized methionine, deamidation, chemical artifacts and non-permitted residues for each modification were not considered. For the amino acid distributions E-H, only modification-amino acid pairs significantly enriched at an adjusted significance level (q<0.01) after a binomial test were included.

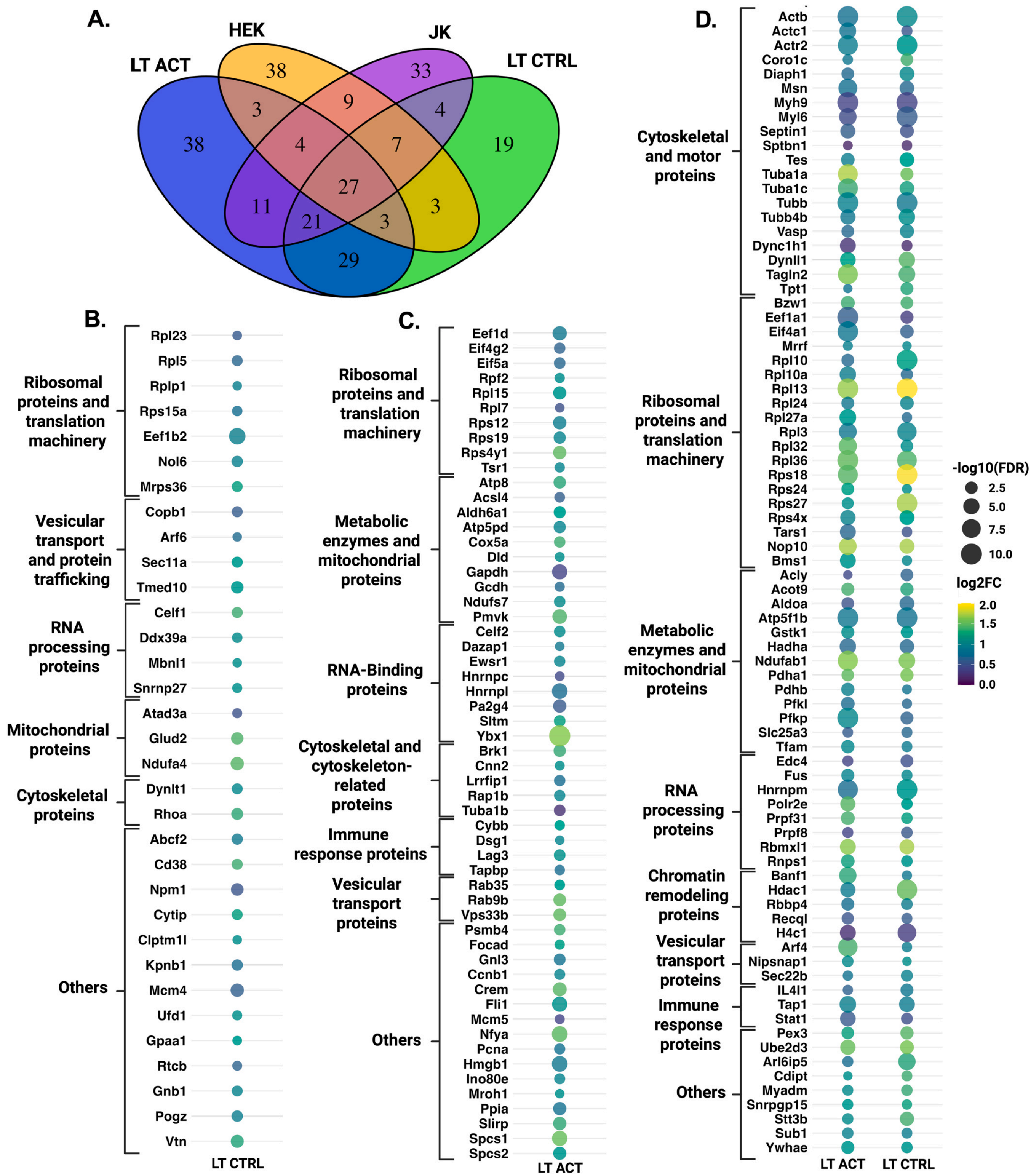

Fig. 2. Proteins significantly enriched in oxidative PTMs. A. Venn diagram showing overlap of proteins significantly enriched in oxidative PTMs across JK (in purple), HEK (in orange), LT CTRL (in green) and LT ACT (in blue) proteomes. **B-D.** Bubble plots showing the proteins enriched in oxidative PTMs in: **B.** LT CTRL but not in LT ACT centrosome proteome; **C.** LT ACT but not in LT CTRL centrosomal proteome; **D.** LT CTRL and LT ACT centrosome proteome. Proteins are grouped by functional categories. The size of each bubble corresponds to the statistical significance of the enrichment as −log10(FDR), while the color gradient indicates the log fold change (log2FC) of each protein. Fold change (FC) was calculated as the ratio of observed oxidative modification levels to the expected levels, which were determined by the product of protein abundance and the proportion of oxidation within the total proteome.

(2025) [preprint]. This approach utilizes a peptide-centric integration pathway that decomposes quantitative information into separate layers, allowing for the identification of biologically relevant PTM changes while minimizing artifacts. A key component of this analysis involved the normalization of peptidoform quantifications at the peptide level, using the non-modified (NM) peptidoform as a reference. This NM-based correction is essential for distinguishing specific PTM changes, driven by the biology, from technical variations. Using this approach we did not find specific PTM changes when comparing LT ACT with LT CTRL. However, we were able to identify statistically significant differences ($p < 0.05$) in some non-modified peptides, which in the integrative workflow reflect the presence of hypermodified regions (Devesa et al., 2025 [preprint]). The most pronounced were found in myosin heavy chain 9 (Myh9) and granzyme A (Gzma). Myh9 (Fig. 3A) showed two hyperoxidized peptides in LT ACT compared to LT CTRL. In contrast, Gzma showed one peptide that concentrated oxidative modifications that were decreased upon LT activation (Fig. 3B). Remarkably, this zone is within the peptidase S1 domain of Gzma (residues 29–259).

To analyze these findings from a systems biology perspective, we selected the top 60 more hypermodified or hypomodified proteins and performed a functional enrichment analysis (see Material and methods). Notably, proteins from both groups were significantly enriched in RNA binding (GO:0003723), with 39 hypomodified proteins (q-value $= 1.57 \cdot 10^{-23}$) and 29 hypermodified proteins (q-value $= 4.17 \cdot 10^{-12}$) associated with this function (data not shown). Similarly, significant enrichment in the ribonucleoprotein complex (GO:1990904) was observed in both groups but was more pronounced among hypomodified proteins (17 proteins, q-value $= 3.76 \cdot 10^{-9}$) compared to hypermodified proteins

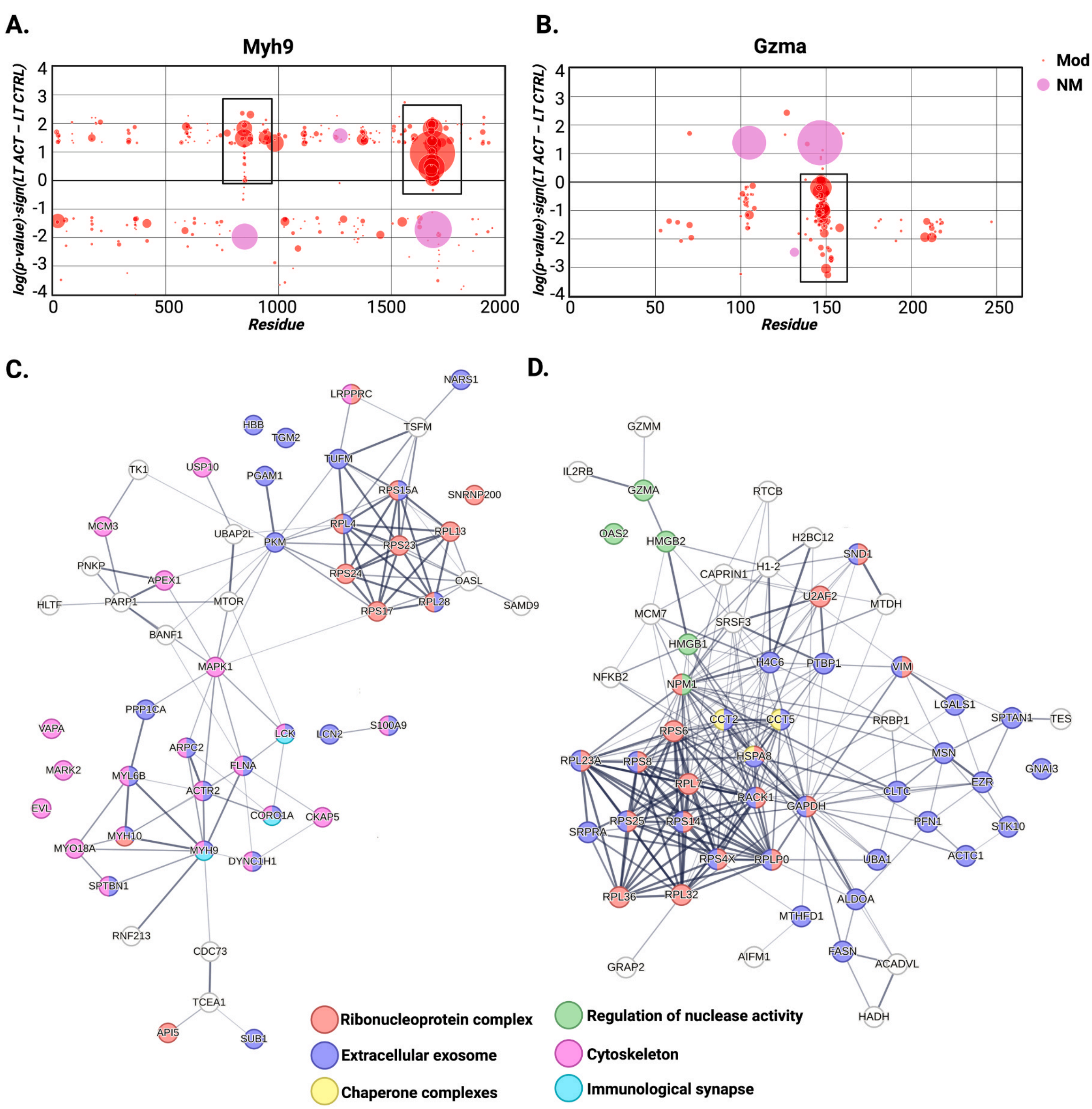

Fig. 3. PTMaps of Myh9 and Gzma. A. PTMap of myosin heavy chain 9 (Myh9). The black rectangles highlight two hyperoxidized regions within the protein sequence. **B.** PTMap of granzyme A (Gzma). The black rectangle highlights a hypooxidized region within the protein sequence. **C.** STRING protein-protein interaction network of hypermodified proteins in LT ACT vs LT CTRL. **D.** STRING protein-protein interaction network of hypomodified proteins in LT ACT vs LT CTRL. PTMaps (A-B) illustrate the distribution of PTMs that showed significant differences (one-sample Limma p-value < 0.05) in LT ACT compared with LT CTRL. The x-axis represents the amino acid residue position in the protein sequence, while the y-axis shows the significance of the relative abundance change in PTMs between two conditions, expressed as log(p-value)·sign(LT ACT – LT CTRL). Each circle corresponds to a specific modification at a residue, with the circle size reflecting the relative frequency of the modification based on peptide spectral matches (PSMs). Red circles indicate modified residues (Mod), while purple circles represent their non-modified versions (NM). In the STRING networks (C-D) the different functional categories are colored as indicated in the graph.

(11 proteins, q-value = 0.00042) (Fig. 3C-D). Another shared feature was the enrichment in extracellular exosome (GO:0070062) proteins, with 29 hypomodified (q-value = $2.84 \cdot 10^{-10}$) and 23 hypermodified (q-value = $4.1 \cdot 10^{-6}$) proteins classified under this category (Fig. 3C-D). Despite these similarities, distinct GO enrichments were observed between the two groups. Hypomodified proteins were significantly associated with chaperone complexes (GO:0101031) (3 proteins, q-value = 0.0165) and regulation of nuclease activity (GO:0032069) (5 proteins, q-value = $6.36 \cdot 10^{-5}$) (Fig. 3C-D). Interestingly, not only granzyme A (Gzma) but also granzyme M (Gzmm) were part of the regionally hypomodified group of proteins. In contrast, hypermodified proteins were enriched in cytoskeletal components (GO:0005856) (21 proteins, q-value = 0.00025) and were significantly associated with the immunological synapse (GO:0001772) (3 proteins, q-value = 0.0130) (Fig. 3C-D), a critical structure for T cell activation. These findings suggest that regionally hyper- or hypomodified proteins are non-randomly distributed across functional pathways.

5. Discussion

This study provides the first comprehensive mapping of PTMs in the T cell centrosome proteome, highlighting the dynamic changes that occur during T cell activation. By employing novel bioinformatics tools (Bagwan et al., 2018; García-Marqués et al., 2016; Rodríguez et al., 2023; Devesa et al., 2025 [preprint]), we identified a diverse array of PTMs, with oxidative modifications being the most prevalent across different cell types—including Jurkat (JK) E6–1 human T cells, human embryonic kidney (HEK) 293 cells, and both resting (LT CTRL) and activated human T lymphoblasts (LT ACT).

Our findings demonstrate that oxidative PTMs constitute the majority of modifications in the centrosome proteome, encompassing various forms such as mono-oxidation, di-oxidation, tri-oxidation, and specific derivatives like kynurenine. Notably, Trp residues emerged as the most frequently oxidized amino acids, exhibiting up to seven distinct types of oxidative modifications. This prevalence underscores the susceptibility of Trp to oxidative processes (Ehrenshaft et al., 2015; Bellmaine et al., 2020) and suggests a significant role for oxidative modifications in regulating centrosomal protein function. The similarity in PTM profiles among different cell types suggests that centrosomal proteins are inherently prone to oxidative modifications, potentially reflecting fundamental aspects of centrosome biology.

Further analysis revealed that the proteins significantly enriched in oxidative PTMs in LT CTRL and/or LT ACT proteomes are involved in key cellular functions, including translation machinery proteins (e.g., ribosomal proteins Rpl23, Rps19; translation factors Eef1a1, Eif4a1), vesicular trafficking proteins (e.g., Rab35, Sec22b), RNA binding and/or processing proteins (e.g., Polr2e, Ddx39a), mitochondrial proteins (e.g., Atad3a, Tfam), cytoskeleton proteins (e.g., Actb, Myh9), immune response proteins (e.g., IL4I1) and chromatin remodeling proteins (e.g., Hdac1). The overlapping set of proteins in both proteomes indicates that oxidative modifications of centrosomal proteins are a conserved feature and may be crucial for its function. However, the presence of proteins uniquely enriched in oxidative PTMs in LT CTRL or LT ACT centrosome proteomes implies that certain oxidative PTMs are regulated, possibly reflecting differences in cellular oxidative environments or metabolic states, which are known to shift upon T cell activation (Shu et al., 2023).

A particularly interesting observation from our study is the differential regulation of certain PTMs, such as kynurenine formation, in specific proteins upon T cell activation. Kynurenine is a product of the oxidative degradation of Trp, often resulting from oxidative stress or enzymatic activity (e.g. indoleamine 2,3-dioxygenase (IDO) activity) under physiological conditions, primarily in response to inflammatory signals like interferon-gamma (IFN-γ). Kynurenine and its metabolites are known to play significant roles in immune regulation, influencing T cell proliferation, differentiation, and function (Puccetti and Grohmann, 2007; Platten et al., 2019; Chen et al., 2024), acting as immunosuppressive agents and inducing regulatory T cells (Stone and Williams, 2023; Munn and Mellor, 2016). However, IDO acts specifically on free L-Trp molecules and there is no evidence to suggest that IDO's active site can act on protein-incorporated Trp residues. Trp residues within proteins can be oxidized to kynurenine and other derivatives through non-enzymatic processes involving reactive oxygen species (ROS) or reactive nitrogen species (RNS). While research specifically focusing on protein-bound kynurenine is limited, this PTM and other oxidized Trp residues have the potential to impact immune responses. The oxidation of Trp to kynurenine introduces a carbonyl group and alters the side chain's properties, which disrupts bonding that is essential for maintaining protein structure (Shields et al., 2021; Cai and Yan, 2013). These conformational changes could further alter protein stability and lead to protein misfolding (Bellmaine et al., 2020). Thus, protein function and its interactions with other proteins and molecules could be affected. Additionally, oxidative stress and redox signaling are closely linked to immune function (Shu et al., 2023; Yarosz and Chang, 2018; Peng et al., 2021). The presence of oxidized amino acids like kynurenine within proteins may serve as signals for redox-sensitive pathways, influencing immune cell activation, differentiation, or apoptosis. The localized regulation of kynurenine modifications within proteins suggests a mechanism by which T cells can finely adjust their activation states and effector functions without altering systemic levels of kynurenine metabolites.

In our analysis, we found that myosin heavy chain 9 (Myh9) exhibited zones with increased levels of oxidation, including kynurenine, in activated T lymphoblasts compared to resting T cells. Myosins are motor proteins critical for cytoskeletal dynamics, cell motility, and the formation of the immune synapse during T cell activation. Thus, they are essential for T cells to form stable contacts with antigen-presenting cells and to initiate downstream signaling pathways (Garrido-Casado et al., 2021; Vicente-Manzanares and Sánchez-Madrid, 2004; Fritzsche et al., 2017). Such modifications might modulate their ATPase activity or binding affinity to actin, thereby influencing cellular processes like migration and immune synapse formation through an enhancement of cytoskeletal dynamics.

Remarkably, we observed that granzyme A (Gzma) exhibited another region that was extensively modified including kynurenine and mono-oxidation among other oxidative PTMs, being all of them decreased in activated T lymphoblasts. Gzma is a serine protease stored in the granules of cytotoxic CD8 T lymphocytes and natural killer cells, playing a crucial role in inducing apoptosis in target cells (Aubert et al., 2024). Gzma expression in CD4 T cells plays a critical role in modulating immune responses and has been associated with both protective and pathological outcomes, particularly in the context of cancer, autoimmune diseases, and chronic infections. Additionally, Gzma expression is tightly regulated during immune activation. Evidence suggests that Gzma is frequently upregulated in CD4 T cells within inflamed tissues, likely because of T cell receptor (TCR) activation, and that CD4 T cells release granzymes upon this stimulation. Moreover, granzyme A has been implicated in non-cytolytic inflammatory processes, such as the induction of pro-inflammatory cytokines, including IL-1β and IL-18. The role of granzyme A-producing CD4 T cells in contributing to tissue damage in autoimmune diseases highlights the significance of Gzma regulation as a critical factor in the pathological activity of CD4 T cells during immune responses (Park et al., 2021). The reduction in oxidative modifications upon activation may enhance granzyme A's stability and/or enzymatic activity. Indeed, the hypomodified zone of granzyme A is within its peptidase S1 domain (residues 29–259). Therefore, the alterations in the pattern of modifications in this zone in granzyme A could facilitate and/or tune-up its function during immune responses, contributing to the effective elimination of infected or malignant cells.

The predominance of oxidative PTMs in centrosomal proteins highlights the potential role of ROS in modulating centrosome function and aligns with previous studies indicating that ROS levels increase during T cell activation (Shu et al., 2023). The differential regulation of oxidative

PTMs such as kynurenine in Myh9 and Gzma suggests these modifications are not merely byproducts of cellular oxidative stress but may serve as regulatory mechanisms fine-tuning protein function during T cell activation. This aligns with the concept that controlled oxidative environments influence various cellular signaling pathways, and ROS can act as secondary messengers modulating immune responses (Yarosz and Chang, 2018; Peng et al., 2021). The balance between oxidation and reduction states of proteins is critical for maintaining cellular homeostasis and function. In this case, enhanced oxidation of myosins may promote the dynamic cytoskeletal changes necessary for T cell proliferation, migration, and interaction with antigen-presenting cells, while the decreased oxidation of granzyme A may ensure its effectiveness in executing cytotoxic functions.

Our analysis reveals a non-random distribution of hypermodified and hypomodified proteins across functional pathways, suggesting that PTM remodeling is an important regulatory mechanism during T cell activation. The shared enrichment of both hypermodified and hypomodified proteins in RNA-binding, ribonucleoprotein complex, and exosome proteins reflect the PTM role in post-transcriptional regulation (e.g., mRNA stability, splicing), as well as their involvement in translation and intercellular communication via extracellular vesicles, respectively. Additionally, hypermodified proteins showed a distinct association with cytoskeletal components, which play a key role in immunological synapse formation (Vicente-Manzanares and Sánchez-Madrid, 2004; Fritzsche et al., 2017; Martín-Cófreces et al., 2014) – cellular component that also appeared as enriched in this analysis. On the other hand, hypomodified proteins were uniquely enriched in chaperone complexes and nuclease activity regulatory proteins, and both proteases Gzma and Gzmm were present in this subgroup.

The preferential hypermodification may be explained by ROS-mediated oxidation. As discussed above, T cell activation generates ROS as a byproduct of metabolic reprogramming (Peng et al., 2021), which could lead to oxidative modifications in a subset of proteins. This raises the question of why certain cytoskeletal proteins are particularly susceptible to hypermodification—potentially due to their abundance, exposure, or intrinsic sensitivity to oxidative stress. Alternatively, these modifications could be functionally relevant, contributing to cytoskeletal reorganization required for T cell activation and effector functions. Hypomodification of specific proteins could reflect changes in subcellular localization, structural remodeling or chromatin dynamics. Another plausible hypothesis is an increased protein turnover, with newly synthesized proteins lacking modifications. This aligns with the idea that PTM removal may serve as a reset mechanism, allowing proteins to regain full activity or undergo targeted degradation during T cell activation (Lee et al., 2023). Moreover, these results potentially align with what has been described in the different T cell activation states. In effector cells, glycolysis and elevated ROS favor hyperoxidation of immunological synapse and cytoskeletal proteins, supporting rapid actin remodeling, synapse stabilization, and directed vesicle secretion (Sena et al., 2013; Wurzer et al., 2019; Buck et al., 2016). Conversely, memory cells rely on fatty acid oxidation and oxidative phosphorylation with attenuated ROS at rest, which would reduce oxidation at these sites, while post-transcriptional control by RNA-binding proteins maintains a poised program for rapid recall (Buck et al., 2016; Hoefig et al., 2021; Cook et al., 2022; Salerno et al., 2018). Consistent with this framework, the hypomodification we observe across chaperone and nuclease regulators and over Gzma and Gzmm is compatible with selective removal of inhibitory oxidative PTMs to enhance catalytic ability during acute effector responses, and with the lower basal granzyme content typical of conventional memory CD4 T cell populations at rest (Grossman et al., 2004; Chattopadhyay et al., 2009).

Taken together, our study contributes to a better understanding of the molecular mechanisms driving immune responses and highlight the potential of targeting specific PTMs to modulate immune function. We emphasize that the functional and mechanistic implications discussed above are hypotheses generated by a descriptive proteomic map and require targeted experimentation beyond the scope of the present work. Moving forward, it would be valuable to explore whether these modifications result from increased ROS production and to investigate the mechanisms leading to the differential regulation of kynurenine modifications upon T cell activation. For example, a comparative analysis of targeted MS (Peterson et al., 2012; van Bentum and Selbach, 2021) of the peptides that were the most enriched in oxidative PTMs (including kynurenine) in resting versus activated primary human T cells could be performed under defined conditions involving the presence or absence of: i) antioxidants (e.g., N-acetyl cysteine (NAC), mitoTEMPO) (Scheffel et al., 2016; Dikalova et al., 2010); ii) ROS boosters (e.g., menadione, antimycin A) (Loor et al., 2010; Quinlan et al., 2011); iii) selective IDO1 inhibitors (e.g., epacadostat) (Yue et al., 2017). In parallel, quantification of extracellular kynurenine metabolites by HPLC would be informative.

To investigate functional consequences, “oxidation resistant” mutagenesis could be employed in proteins with clear Trp oxidation enrichment (particularly, kynurenine enrichment analysis data is in Supplementary Table 3). Since Trp to Phe is considered a conservative substitution (Betts and Russell, 2003), and Phe is less susceptible to oxidation (Hawkins and Davies, 2019; Ehrenshaft et al., 2015), Trp to Phe substitutions at mapped Trp oxidative hotspots could serve as a solid preliminary model to assess if protein specific functions change (e.g., for myosins, immune synapse organization and cytoskeletal dynamics). In the case of Gzma, primary CD4⁺ (or CD8⁺) T cells could be activated and treated with ROS boosters or antioxidants as mentioned above. Lysates and supernatants could be collected, enzymatic activity quantified (Cheng et al., 2023), and oxidation state measured by targeted MS (van Bentum and Selbach, 2021) over the hypomodified region to test whether there are correlations between activity and oxidation states in the different conditions. Lastly, to explore intercellular handling of oxidized species, extracellular vesicles (EVs) could be isolated from LT CTRL and LT ACT supernatants, and subjected to targeted MS. Enrichment of the oxidized peptides in EVs would support a model of redox influenced communication and/or clearance (Welsh et al., 2024; Chiaradia et al., 2021).

Further research into the functional implications of these modifications may pave the way for novel therapeutic strategies in immune-related diseases such as cancer and autoimmunity. A targeted MS biomarker built as a minimal peptide panel (a potential “centrosome redox index”) quantified by parallel reaction monitoring (PRM) or selected reaction monitoring (SRM) could track centrosome redox state during T cell activation in sorted T cells and in EVs (Shi et al., 2016; van Bentum and Selbach, 2021). Selection of concrete oxidized peptides (e.g., from Myh9 and other cytoskeleton proteins along with Gzma S1-domain peptides) would enable a single composite readout of centrosomal redox state and cytotoxic potential. For instance, in autoimmunity, dimethyl fumarate (DMF) (an approved oral electrophile that covalently modifies KEAP1 cysteines to stabilize NRF2 and thus induce an antioxidant program (Baird and Yamamoto, 2020; Brennan et al., 2015)) provides an opportunity to test whether reducing centrosome oxidation attenuates effector activity. Phase-3 trials already establish DMF’s clinical efficacy and safety in multiple sclerosis (Gold et al., 2012; Fox et al., 2012). Of course, this example relies on two assumptions: that Myh9 hyperoxidation attenuates actomyosin contractility, thereby stabilizing the immunological synapse by limiting premature retraction; and that reduced oxidation within the Gzma peptidase S1 domain enhances catalytic competence, which both should be tested in dedicated mechanistic studies (as for the other proteins, if included in the index). At any rate, to examine whether changes in the proposed redox index correlate with clinical improvement would be of great interest.

In this regard, many solid tumors produce ROS that can impair T cell function (Weinberg et al., 2019; Chen et al., 2016). GKT137831 (setanaxib), the first dual NOX1/NOX4 inhibitor to reach clinical trials, is being evaluated in combination with pembrolizumab (anti-PD-1) in recurrent or metastatic head-and-neck squamous cell carcinoma (Thannickal et al., 2023; Fayette et al., 2024). The proposed "centrosome redox index" could be measured in peripheral T cells and plasma EVs as a pharmacodynamic endpoint. Assuming the above, a normalization of the index in responders would be expected, consistent with an improved immune response performance. This framework is further supported by reversible redox control of cytoskeletal dynamics at the synapse via the MICAL-MsrB system (Lee et al., 2013; Hung et al., 2013). However, as in the previous example, regardless of the specific results, these clinical settings would provide relevant mechanistic insights into the underlying biological mechanisms.

Altogether, our study deepens understanding of T cell activation and highlights centrosomal PTMs, particularly ROS-linked changes, as promising targets to modulate T cell function.

CRediT authorship contribution statement

Inmaculada Jorge: Writing – original draft, Validation, Formal analysis, Data curation. **Emilio Camafeita:** Writing – original draft, Validation, Formal analysis, Data curation. **Cristina A. Devesa:** Software. **Rafael Barrero-Rodríguez:** Software. **Enrique Calvo:** Formal analysis, Data curation. **Andrea Laguillo-Gómez:** Software. **Clara Pertusa:** Data curation. **Noa B. Martin-Cofreces:** Writing – original draft, Supervision, Funding acquisition, Conceptualization. **Jesús Vázquez:** Writing – original draft, Supervision, Funding acquisition, Conceptualization. **Francisco Sánchez-Madrid:** Writing – original draft, Supervision, Funding acquisition, Conceptualization. **Marta Lozano-Prieto:** Writing – original draft, Validation, Formal analysis, Data curation.

Declaration of Competing Interest

The authors declare that they have no known competing financial interests or personal relationships that could have appeared to influence the work reported in this paper.

Acknowledgements

This study was supported by the Spanish Ministry of Science and Innovation, Agencia Estatal de Investigación by competitive grants PID2023–149541OB-I00, PID2022–141890B-I00, PID2020–120412RB-I00, PDC2021–121797-I00 and PID2021–122348NB-I00 funded by MICIU/AEI/ 10.13039/501100011033 and by "ERDF A way of making Europe", PLEC2022–009298, PLEC2022–009235 and EQC2021–007053-P funded by MICIU/AEI/10.13039/501100011033 and by "European Union NextGenerationEU/ PRTR", and S2022/BMD-7333-CM (INMUNOVAR-CM) and P2022/BMD7209 (INTEGRAMUNE) funded by Comunidad de Madrid. CIBER Cardiovascular (CB16/11/00272, CB16/11/00277) Fondo de Investigación Sanitaria del Instituto de Salud Carlos III; co-funding by Fondo Europeo de Desarrollo Regional (FEDER). The project leading to these results has received funding from "La Caixa" Foundation under the project codes LCF/PR/HR22/52420019 and LCF/PR/HR23/52430018. MLP is supported by a FPI fellowship (PRE2021–097478). ALG is supported by a FPU fellowship (FPU18/03882). RBR is supported by a FPU fellowship (FPU20/03365). CAD is supported by a FPI fellowship (PRE2019–090019). The CNIC is supported by the Instituto de Salud Carlos III (ISCIII), the Ministerio de Ciencia, Innovación Y Universidades (MICIU) and the Pro CNIC Foundation), and is a Severo Ochoa Center of Excellence (grant CEX2020–001041-S funded by MICIU/AEI/10.13039/501100011033).

Ethics Statement

Samples were isolated from buffy coat preparations from healthy donors provided by Centro de Transfusiones de la Comunidad de Madrid under an agreement with the IIS-Princesa (Madrid, Spain) in accordance with the Declaration of Helsinki and the government ethical consent, and approved by the Hospital La Princesa Research Ethics Committee.

Appendix A. Supporting information

Supplementary data associated with this article can be found in the online version at doi:10.1016/j.ejcb.2025.151521.

Data availability

The MS proteomics data have been deposited to the ProteomeXchange Consortium via the PRIDE partner repository, as indicated in the manuscript.

References

Alquezar, C., Arya, S., Kao, A.W., 2021. Tau Post-translational modifications: dynamic transformers of tau function, degradation, and aggregation. Front. Neurol. 11, 595532. https://doi.org/10.3389/fneur.2020.595532.

Aubert, A., Jung, K., Hiroyasu, S., Pardo, J., Granville, D.J., 2024. Granzyme serine proteases in inflammation and rheumatic diseases. Nat. Rev. Rheumatol. 20 (6), 361–376. https://doi.org/10.1038/s41584-024-01109-5.

Bagwan, N., Bonzon-Kulichenko, E., Calvo, E., Lechuga-Vieco, A.V., Michalakopoulos, S., Trevisan-Herraz, M., Ezkurdia, I., Rodríguez, J.M., Magni, R., Latorre-Pellicer, A., et al., 2018. Comprehensive quantification of the modified proteome reveals oxidative heart damage in mitochondrial heteroplasmy. .e4 Cell Rep. 23 (12), 3685–3697. https://doi.org/10.1016/j.celrep.2018.05.080.

Baird, L., Yamamoto, M., 2020. The molecular mechanisms regulating the KEAP1-NRF2 pathway. e00099-20 Mol. Cell. Biol. 40 (13). https://doi.org/10.1128/MCB.00099-20.

Bellmaine, S., Schnellbaecher, A., Zimmer, A., 2020. Reactivity and degradation products of tryptophan in solution and proteins. Free Radic. Biol. Med. 160, 696–718. https://doi.org/10.1016/j.freeradbiomed.2020.09.002.

van Bentum, M., Selbach, M., 2021. An introduction to advanced targeted acquisition methods. Mol. Cell. Proteom. MCP 20, 100165. https://doi.org/10.1016/j.mcpro.2021.100165.

Betts, M.J., Russell, R.B., 2003. Amino acid properties and consequences of substitutions. In: Barnes, M.R., Gray, I.C. (Eds.), In Bioinformatics for Geneticists. https://doi.org/10.1002/0470867302.ch14.

Binek, A., Castans, C., Jorge, I., Bagwan, N., Rodríguez, J.M., Fernández-Jiménez, R., Galán-Arriola, C., Oliver, E., Gómez, M., Clemente-Moragón, A., et al., 2024. Oxidative Post-translational protein modifications upon Ischemia/Reperfusion injury. Antioxidants (Basel) 13 (1), 106. https://doi.org/10.3390/antiox13010106.

Brennan, M.S., Matos, M.F., Li, B., Hronowski, X., Gao, B., Juhasz, P., Rhodes, K.J., Scannevin, R.H., 2015. Dimethyl fumarate and monoethyl fumarate exhibit differential effects on KEAP1, NRF2 activation, and glutathione depletion in vitro. PloS One 10 (3), e0120254. https://doi.org/10.1371/journal.pone.0120254.

Buck, M.D., O'Sullivan, D., Klein Geltink, R.I., Curtis, J.D., Chang, C.H., Sanin, D.E., Qiu, J., Kretz, O., Braas, D., van der Windt, G.J., et al., 2016. Mitochondrial dynamics controls t cell fate through metabolic programming. Cell 166 (1), 63–76. https://doi.org/10.1016/j.cell.2016.05.035.

Cai, Z., Yan, L.J., 2013. Protein oxidative modifications: beneficial roles in disease and health. J. Biochem. Pharmacol. Res. 1 (1), 15–26.

Cano-Gamez, E., Soskic, B., Roumeliotis, T.I., So, E., Smyth, D.J., Baldrighi, M., Willé, D., Nakic, N., Esparza-Gordillo, J., Larminie, C.G.C., et al., 2020. Single-cell transcriptomics identifies an effectorness gradient shaping the response of CD4+ t cells to cytokines. Nat. Commun. 11 (1), 1801. https://doi.org/10.1038/s41467-020-15543-y.

Chattopadhyay, P.K., Betts, M.R., Price, D.A., Gostick, E., Horton, H., Roederer, M., De Rosa, S.C., 2009. The cytolytic enzymes granyzme A, granzyme B, and perforin: expression patterns, cell distribution, and their relationship to cell maturity and bright CD57 expression. J. Leukoc. Biol. 85 (1), 88–97. https://doi.org/10.1189/jlb.0208107.

Chen, E., Wu, J., Huang, J., Zhu, W., Sun, H., Wang, X., Lin, D., Li, X., Shi, D., Liu, Z., et al., 2024. FLI1 promotes IFN-γ-induced kynurenine production to impair anti-tumor immunity. Nat. Commun. 15 (1), 4590. https://doi.org/10.1038/s41467-024-48397-9.

Chen, X., Song, M., Zhang, B., Zhang, Y., 2016. Reactive oxygen species regulate t cell immune response in the tumor microenvironment. Oxid. Med. Cell. Longev. 2016, 1580967. https://doi.org/10.1155/2016/1580967.

Cheng, Z., Thompson, E.J., Mendive-Tapia, L., Scott, J.I., Benson, S., Kitamura, T., Senan-Salinas, A., Samarakoon, Y., Roberts, E.W., Arias, M.A., et al., 2023. Fluorogenic granzyme a substrates enable Real-Time imaging of adaptive immune cell activity. Angew. Chem. (Int. Ed. Engl.) 62 (8), e202216142. https://doi.org/10.1002/anie.202216142.

Chiaradia, E., Tancini, B., Emiliani, C., Delo, F., Pellegrino, R.M., Tognoloni, A., Urbanelli, L., Buratta, S., 2021. Extracellular vesicles under oxidative stress conditions: biological properties and physiological roles. Cells 10 (7), 1763. https://doi.org/10.3390/cells10071763.

Chick, J.M., Kolippakkam, D., Nusinow, D.P., Zhai, B., Rad, R., Huttlin, E.L., Gygi, S.P., 2015. A mass-tolerant database search identifies a large proportion of unassigned

spectra in shotgun proteomics as modified peptides. Nat. Biotechnol. 33 (7), 743–749. https://doi.org/10.1038/nbt.3267.
Cook, M.E., Bradstreet, T.R., Webber, A.M., Kim, J., Santeford, A., Harris, K.M., Murphy, M.K., Tran, J., Abdalla, N.M., Schwarzkopf, E.A., et al., 2022. The ZFP36 family of RNA binding proteins regulates homeostatic and autoreactive t cell responses. Sci. Immunol. 7 (76), eabo0981. https://doi.org/10.1126/sciimmunol.abo0981.
[preprint]Devesa, C.A., Barrero-Rodríguez, R., Laguillo-Gómez, A., Guerrero-Sánchez, V. M., del Río-Aledo, D., Mena, D., Jorge, I., Núñez, E., Calvo, E., López, J.A., et al. Integrative multi-layer workflow for quantitative analysis of post-translational modifications. bioRxiv. 2025. https://doi.org/10.1101/2025.01.20.633864.
Dikalova, A.E., Bikineyeva, A.T., Budzyn, K., Nazarewicz, R.R., McCann, L., Lewis, W., Harrison, D.G., Dikalov, S.I., 2010. Therapeutic targeting of mitochondrial superoxide in hypertension. Circ. Res. 107 (1), 106–116. https://doi.org/10.1161/CIRCRESAHA.109.214601.
Dybas, J.M., O'Leary, C.E., Ding, H., Spruce, L.A., Seeholzer, S.H., Oliver, P.M., 2019. Integrative proteomics reveals an increase in non-degradative ubiquitylation in activated CD4+ t cells. Nat. Immunol. 20 (6), 747–755. https://doi.org/10.1038/s41590-019-0381-6.
Ehrenshaft, M., Deterding, L.J., Mason, R.P., 2015. Tripping up trp: modification of protein tryptophan residues by reactive oxygen species, modes of detection, and biological consequences. Free Radic. Biol. Med. 89, 220–228. https://doi.org/10.1016/j.freeradbiomed.2015.08.003.
Fayette, J., Thomas, G., Daste, A., Rotarski, M., Castelo, B., Rullan, A., Levine, A., Philipson, R.S., Harrington, K.J., 2024. 853MO setanaxib plus pembrolizumab for the treatment of recurrent or metastatic squamous cell carcinoma of the head & neck: results of a randomized, double-blind phase II trial. Ann. Oncol. 35 (2), S615–S616. https://doi.org/10.1016/j.annonc.2024.08.914.
Fox, R.J., Miller, D.H., Phillips, J.T., Hutchinson, M., Havrdova, E., Kita, M., Yang, M., Raghupathi, K., Novas, M., Sweetser, M.T., et al., 2012. Placebo-controlled phase 3 study of oral BG-12 or glatiramer in multiple sclerosis. N. Engl. J. Med. 367 (12), 1087–1097. https://doi.org/10.1056/NEJMoa1206328.
Fritzsche, M., Fernandes, R.A., Chang, V.T., Colin-York, H., Clausen, M.P., Felce, J.H., Galiani, S., Erlenkämper, C., Santos, A.M., Heddleston, J.M., et al., 2017. Cytoskeletal actin dynamics shape a ramifying actin network underpinning immunological synapse formation. Sci. Adv. 3 (6), e1603032. https://doi.org/10.1126/sciadv.1603032.
de la Fuente-Alonso, A., Toral, M., Alfayate, A., Ruiz-Rodríguez, M.J., Bonzón-Kulichenko, E., Teixido-Tura, G., Martínez-Martínez, S., Méndez-Olivares, M.J., López-Maderuelo, D., González-Valdés, I., et al., 2021. Aortic disease in marfan syndrome is caused by overactivation of sGC-PRKG signaling by NO. Nat. Commun. 12 (1), 2628. https://doi.org/10.1038/s41467-021-22933-3.
García-Marqués, F., Trevisan-Herraz, M., Martínez-Martínez, S., Camafeita, E., Jorge, I., Lopez, J.A., Méndez-Barbero, N., Méndez-Ferrer, S., Del Pozo, M.A., Ibáñez, B., et al., 2016. A novel Systems-Biology algorithm for the analysis of coordinated protein responses using quantitative proteomics. Mol. Cell Proteom. 15 (5), 1740–1760. https://doi.org/10.1074/mcp.M115.055905.
Garrido-Casado, M., Asensio-Juárez, G., Vicente-Manzanares, M., 2021. Nonmuscle myosin II regulation directs its multiple roles in cell migration and division. Annu Rev. Cell Dev. Biol. 37, 285–310. https://doi.org/10.1146/annurev-cellbio-042721-105528.
Geha, R., Rosen, F., Merler, E., 1974. Unresponsiveness of human b lymphocytes to phytohaemagglutinin. Nature 248, 426–428. https://doi.org/10.1038/248426a0.
Gold, R., Kappos, L., Arnold, D.L., Bar-Or, A., Giovannoni, G., Selmaj, K., Tornatore, C., Sweetser, M.T., Yang, M., Sheikh, S.I., et al., 2012. Placebo-controlled phase 3 study of oral BG-12 for relapsing multiple sclerosis. N. Engl. J. Med. 367 (12), 1098–1107. https://doi.org/10.1056/NEJMoa1114287.
Grossman, W.J., Verbsky, J.W., Tollefsen, B.L., Kemper, C., Atkinson, J.P., Ley, T.J., 2004. Differential expression of granzymes a and b in human cytotoxic lymphocyte subsets and t regulatory cells. Blood 104 (9), 2840–2848. https://doi.org/10.1182/blood-2004-03-0859.
Hawkins, C.L., Davies, M.J., 2019. Detection, identification, and quantification of oxidative protein modifications. J. Biol. Chem. 294 (51), 19683–19708. https://doi.org/10.1074/jbc.REV119.006217.
Hoefig, K.P., Reim, A., Gallus, C., Wong, E.H., Behrens, G., Conrad, C., Xu, M., Kifinger, L., Ito-Kureha, T., Defourny, K.A.Y., et al., 2021. Defining the RBPome of primary t helper cells to elucidate higher-order Roquin-mediated mRNA regulation. Nat. Commun. 12 (1), 5208. https://doi.org/10.1038/s41467-021-25345-5.
Howden, A.J.M., Hukelmann, J.L., Brenes, A., Spinelli, L., Sinclair, L.V., Lamond, A.I., Cantrell, D.A., 2019. Quantitative analysis of t cell proteomes and environmental sensors during t cell differentiation. Nat. Immunol. 20 (11), 1542–1554. https://doi.org/10.1038/s41590-019-0495-x.
Hulstaert, N., Shofstahl, J., Sachsenberg, T., Walzer, M., Barsnes, H., Martens, L., Perez-Riverol, Y., 2020. ThermoRawFileParser: modular, scalable, and Cross-Platform RAW file conversion. J. Proteome Res. 19 (1), 537–542. https://doi.org/10.1021/acs.jproteome.9b00328.
Hung, R.J., Spaeth, C.S., Yesilyurt, H.G., Terman, J.R., 2013. SelR reverses Mical-mediated oxidation of actin to regulate F-actin dynamics. Nat. Cell Biol. 15 (12), 1445–1454. https://doi.org/10.1038/ncb2871.
Junqueira, S.C., Centeno, E.G.Z., Wilkinson, K.A., Cimarosti, H., 2019. Post-translational modifications of parkinson's disease-related proteins: phosphorylation, SUMOylation and ubiquitination. Biochim Biophys. Acta Mol. Basis Dis. 1865 (8), 2001–2007. https://doi.org/10.1016/j.bbadis.2018.10.025.
Jurgens, A.P., Popović, B., Wolkers, M.C., 2021. T cells at work: how post-transcriptional mechanisms control t cell homeostasis and activation. Eur. J. Immunol. 51 (9), 2178–2187. https://doi.org/10.1002/eji.202049055.
Kennell, A.S., Gould, K.G., Salaman, M.R., 2014. Proliferation assay amplification by IL-2 in model primary and recall antigen systems. BMC Res. Notes 7, 662. https://doi.org/10.1186/1756-0500-7-662.
Laguillo-Gómez, A., Calvo, E., Martín-Cófreces, N., Lozano-Prieto, M., Sánchez-Madrid, F., Vázquez, J., 2023. ReCom: a semi-supervised approach to ultra-tolerant database search for improved identification of modified peptides. J. Proteom. 287, 104968. https://doi.org/10.1016/j.jprot.2023.104968.
Lechuga-Vieco, A.V., Latorre-Pellicer, A., Calvo, E., Torroja, C., Pellico, J., Acín-Pérez, R., García-Gil, M.L., Santos, A., Bagwan, N., Bonzon-Kulichenko, E., et al., 2022. Heteroplasmy of Wild-Type mitochondrial DNA variants in mice causes metabolic heart disease with pulmonary hypertension and frailty. Circulation 145 (14), 1084–1101. https://doi.org/10.1161/CIRCULATIONAHA.121.056286.
Lee, B.C., Péterfi, Z., Hoffmann, F.W., Moore, R.E., Kaya, A., Avanesov, A., Tarrago, L., Zhou, Y., Weerapana, E., Fomenko, D.E., et al., 2013. MsrB1 and MICALs regulate actin assembly and macrophage function via reversible stereoselective methionine oxidation. Mol. Cell 51 (3), 397–404. https://doi.org/10.1016/j.molcel.2013.06.019.
Lee, J.M., Hammarén, H.M., Savitski, M.M., Baek, S.H., 2023. Control of protein stability by post-translational modifications. Nat. Commun. 14 (1), 201. https://doi.org/10.1038/s41467-023-35795-8.
Liu, R., Zeng, L.W., Gong, R., Yuan, F., Shu, H.B., Li, S., 2021. mTORC1 activity regulates post-translational modifications of glycine decarboxylase to modulate glycine metabolism and tumorigenesis. Nat. Commun. 12 (1), 4227. https://doi.org/10.1038/s41467-021-24321-3.
Loor, G., Kondapalli, J., Schriewer, J.M., Chandel, N.S., Vanden Hoek, T.L., Schumacker, P.T., 2010. Menadione triggers cell death through ROS-dependent mechanisms involving PARP activation without requiring apoptosis. Free Radic. Biol. Med. 49 (12), 1925–1936. https://doi.org/10.1016/j.freeradbiomed.2010.09.021.
Lozano-Prieto, M., Camafeita, E., Jorge, I., Laguillo-Gómez, A., Barrero-Rodríguez, R., Devesa, C.A., Pertusa, C., Calvo, E., Sánchez-Madrid, F., Vázquez, J., et al., 2024. In-gel protein digestion using acidic methanol produces a highly selective methylation of glutamic acid residues. J. Proteom. 304, 105229. https://doi.org/10.1016/j.jprot.2024.105229.
Martin-Cofreces, N.B., Chichon, F.J., Calvo, E., Torralba, D., Bustos-Moran, E., Dosil, S. G., Rojas-Gomez, A., Bonzon-Kulichenko, E., Lopez, J.A., Otón, J., et al., 2020. The chaperonin CCT controls t cell receptor-driven 3D configuration of centrioles. Sci. Adv. 6 (49), eabb7242. https://doi.org/10.1126/sciadv.abb7242.
Martín-Cófreces, N.B., Robles-Valero, J., Cabrero, J.R., Mittelbrunn, M., Gordón-Alonso, M., Sung, C.H., Alarcón, B., Vázquez, J., Sánchez-Madrid, F., 2008. MTOC translocation modulates IS formation and controls sustained t cell signaling. J. Cell Biol. 182 (5), 951–962. https://doi.org/10.1083/jcb.200801014.
Martín-Cófreces, N.B., Baixauli, F., Sánchez-Madrid, F., 2014. Immune synapse: conductor of orchestrated organelle movement. Trends Cell Biol. 24 (1), 61–72. https://doi.org/10.1016/j.tcb.2013.09.005.
Martínez-López, D., Camafeita, E., Cedó, L., Roldan-Montero, R., Jorge, I., García-Marqués, F., Gómez-Serrano, M., Bonzon-Kulichenko, E., Blanco-Vaca, F., Blanco-Colio, L.M., et al., 2019. APOA1 oxidation is associated to dysfunctional high-density lipoproteins in human abdominal aortic aneurysm. EBioMedicine 43, 43–53. https://doi.org/10.1016/j.ebiom.2019.04.012.
Munn, D.H., Mellor, A.L., 2016. IDO in the tumor microenvironment: inflammation, Counter-Regulation, and tolerance. Trends Immunol. 37 (3), 193–207. https://doi.org/10.1016/j.it.2016.01.002.
Noels, H., Jankowski, V., Schunk, S.J., Vanholder, R., Kalim, S., Jankowski, J., 2024. Post-translational modifications in kidney diseases and associated cardiovascular risk. Nat. Rev. Nephrol. 20 (8), 495–512. https://doi.org/10.1038/s41581-024-00837-x.
Park, S., Anderson, N.L., Canaria, D.A., Olson, M.R., 2021. Granzyme-Producing CD4 t cells in cancer and autoimmune disease. Immunohorizons 5 (12), 909–917. https://doi.org/10.4049/immunohorizons.2100017.
Peng, H.Y., Lucavs, J., Ballard, D., Das, J.K., Kumar, A., Wang, L., Ren, Y., Xiong, X., Song, J., 2021. Metabolic reprogramming and reactive oxygen species in t cell immunity. Front. Immunol. 12, 652687. https://doi.org/10.3389/fimmu.2021.652687.
Peterson, A.C., Russell, J.D., Bailey, D.J., Westphall, M.S., Coon, J.J., 2012. Parallel reaction monitoring for high resolution and high mass accuracy quantitative, targeted proteomics. Mol. Cell. Proteom. MCP 11 (11), 1475–1488. https://doi.org/10.1074/mcp.O112.020131.
Platten, M., Nollen, E.A.A., Röhrig, U.F., Fallarino, F., Opitz, C.A., 2019. Tryptophan metabolism as a common therapeutic target in cancer, neurodegeneration and beyond. Nat. Rev. Drug Discov. 18 (5), 379–401. https://doi.org/10.1038/s41573-019-0016-5.
Puccetti, P., Grohmann, U., 2007. IDO and regulatory t cells: a role for reverse signalling and non-canonical NF-kappaB activation. Nat. Rev. Immunol. 7 (10), 817–823. https://doi.org/10.1038/nri2163.
Quinlan, C.L., Gerencser, A.A., Treberg, J.R., Brand, M.D., 2011. The mechanism of superoxide production by the antimycin-inhibited mitochondrial Q-cycle. J. Biol. Chem. 286 (36), 31361–31372. https://doi.org/10.1074/jbc.M111.267898.
Ricciardi, S., Manfrini, N., Alfieri, R., Calamita, P., Crosti, M.C., Gallo, S., Müller, R., Pagani, M., Abrignani, S., Biffo, S., 2018. The translational machinery of human CD4 + t cells is poised for activation and controls the switch from quiescence to metabolic remodeling. .e5 Cell Metab. 28 (6), 895–906. https://doi.org/10.1016/j.cmet.2018.08.009.
Rodríguez, J.M., Jorge, I., Martinez-Val, A., Barrero-Rodríguez, R., Magni, R., Núñez, E., Laguillo, A., Devesa, C.A., López, J.A., Camafeita, E., et al., 2023. iSanXoT: a standalone application for the integrative analysis of mass spectrometry-based

quantitative proteomics data. Comput. Struct. Biotechnol. J. 23, 452–459. https://doi.org/10.1016/j.csbj.2023.12.034.

Ruiz-Meana, M., Minguet, M., Bou-Teen, D., Miro-Casas, E., Castans, C., Castellano, J., Bonzon-Kulichenko, E., Igual, A., Rodriguez-Lecoq, R., Vázquez, J., et al., 2019. Ryanodine receptor glycation favors mitochondrial damage in the senescent heart. Circulation 139 (7), 949–964. https://doi.org/10.1161/CIRCULATIONAHA.118.035869.

Salerno, F., Engels, S., van den Biggelaar, M., van Alphen, F.P.J., Guislain, A., Zhao, W., Hodge, D.L., Bell, S.E., Medema, J.P., von Lindern, M., et al., 2018. Translational repression of pre-formed cytokine-encoding mRNA prevents chronic activation of memory t cells. Nat. Immunol. 19 (8), 828–837. https://doi.org/10.1038/s41590-018-0155-6.

Scheffel, M.J., Scurti, G., Simms, P., Garrett-Mayer, E., Mehrotra, S., Nishimura, M.I., Voelkel-Johnson, C., 2016. Efficacy of adoptive T-cell therapy is improved by treatment with the antioxidant N-Acetyl cysteine, which limits Activation-Induced T-cell death. Cancer Res. 76 (20), 6006–6016. https://doi.org/10.1158/0008-5472.CAN-16-0587.

Sena, Li, L.A., Jairaman, S., Prakriya, A., Ezponda, M., Hildeman, T., Wang, D.A., Schumacker, C.R., Licht, P.T., Perlman, J.D., et al., 2013. Mitochondria are required for antigen-specific t cell activation through reactive oxygen species signaling. Immunity 38 (2), 225–236. https://doi.org/10.1016/j.immuni.2012.10.020.

Shi, T., Song, E., Nie, S., Rodland, K.D., Liu, T., Qian, W.J., Smith, R.D., 2016. Advances in targeted proteomics and applications to biomedical research. Proteomics 16 (15-16), 2160–2182. https://doi.org/10.1002/pmic.201500449.

Shields, H.J., Traa, A., Van Raamsdonk, J.M., 2021. Beneficial and detrimental effects of reactive oxygen species on lifespan: a comprehensive review of comparative and experimental studies. Front. Cell Dev. Biol. 9, 628157. https://doi.org/10.3389/fcell.2021.628157.

Shu, P., Liang, H., Zhang, J., Lin, Y., Chen, W., Zhang, D., 2023. Reactive oxygen species formation and its effect on CD4+ t cell-mediated inflammation. Front. Immunol. 14, 1199233. https://doi.org/10.3389/fimmu.2023.1199233.

Stone, T.W., Williams, R.O., 2023. Modulation of t cells by tryptophan metabolites in the kynurenine pathway. Trends Pharmacol. Sci. 44 (7), 442–456. https://doi.org/10.1016/j.tips.2023.04.006.

Tan, H., Yang, K., Li, Y., Shaw, T.I., Wang, Y., Blanco, D.B., Wang, X., Cho, J.H., Wang, H., Rankin, S., et al., 2017. Integrative proteomics and phosphoproteomics profiling reveals dynamic signaling networks and bioenergetics pathways underlying t cell activation. Immunity 46 (3), 488–503. https://doi.org/10.1016/j.immuni.2017.02.010.

Thannickal, V.J., Jandeleit-Dahm, K., Szyndralewiez, C., Török, N.J., 2023. Pre-clinical evidence of a dual NADPH oxidase 1/4 inhibitor (setanaxib) in liver, kidney and lung fibrosis. J. Cell. Mol. Med. 27 (4), 471–481. https://doi.org/10.1111/jcmm.17649.

Trevisan-Herraz, M., Bagwan, N., García-Marqués, F., Rodriguez, J.M., Jorge, I., Ezkurdia, I., Bonzon-Kulichenko, E., Vázquez, J., 2019. SanXoT: a modular and versatile package for the quantitative analysis of high-throughput proteomics experiments. Bioinformatics 35 (9), 1594–1596. https://doi.org/10.1093/bioinformatics/bty815.

Ubersax, J.A., Ferrell, J.E., Jr, 2007. Mechanisms of specificity in protein phosphorylation. Nat. Rev. Mol. Cell Biol. 8 (7), 530–541. https://doi.org/10.1038/nrm2203.

Vicente-Manzanares, M., Sánchez-Madrid, F., 2004. Role of the cytoskeleton during leukocyte responses. Nat. Rev. Immunol. 4 (2), 110–122. https://doi.org/10.1038/nri1268.

Weinberg, F., Ramnath, N., Nagrath, D., 2019. Reactive oxygen species in the tumor microenvironment: an overview. Cancers 11 (8), 1191. https://doi.org/10.3390/cancers11081191.

Welsh, J.A., Goberdhan, D.C.I., O'Driscoll, L., Buzas, E.I., Blenkiron, C., Bussolati, B., Cai, H., Di Vizio, D., Driedonks, T.A.P., Erdbrügger, U., et al., 2024. Minimal information for studies of extracellular vesicles (MISEV2023): from basic to advanced approaches. J. Extracell. vesicles 13 (2), e12404. https://doi.org/10.1002/jev2.12404.

Wolf, T., Jin, W., Zoppi, G., Vogel, I.A., Akhmedov, M., Bleck, C.K.E., Beltraminelli, T., Rieckmann, J.C., Ramirez, N.J., Benevento, M., et al., 2020. Dynamics in protein translation sustaining t cell preparedness. Nat. Immunol. 21 (8), 927–937. https://doi.org/10.1038/s41590-020-0714-5.

Wurzer, H., Hoffmann, C., Al Absi, A., Thomas, C., 2019. Actin cytoskeleton straddling the immunological synapse between cytotoxic lymphocytes and cancer cells. Cells 8 (5), 463. https://doi.org/10.3390/cells8050463.

Yarosz, E.L., Chang, C.H., 2018. The role of reactive oxygen species in regulating t Cell-mediated immunity and disease. Immune Netw. 18 (1), e14. https://doi.org/10.4110/in.2018.18.e14.

Yu, F., Teo, G.C., Kong, A.T., Haynes, S.E., Avtonomov, D.M., Geiszler, D.J., Nesvizhskii, A.I., 2020. Identification of modified peptides using localization-aware open search. Nat. Commun. 11 (1), 4065. https://doi.org/10.1038/s41467-020-17921-y.

Yue, E.W., Sparks, R., Polam, P., Modi, D., Douty, B., Wayland, B., Glass, B., Takvorian, A., Glenn, J., Zhu, W., et al., 2017. INCB24360 (Epacadostat), a highly potent and selective Indoleamine-2,3-dioxygenase 1 (IDO1) inhibitor for Immuno-oncology. ACS Med. Chem. Lett. 8 (5), 486–491. https://doi.org/10.1021/acsmedchemlett.6b00391.